Available online at www.sciencedirect.com

ScienceDirect

Energy Procedia 159 (2019) 340–345

Energy Procedia

www.elsevier.com/locate/procedia

Applied Energy Symposium and Forum, Renewable Energy Integration with Mini/Microgrids, REM 2018, 29–30 September 2018, Rhodes, Greece

Optimal Sizing and Power Sharing of Distributed Hybrid Renewable Energy Systems Considering Socio-Demographic Factors

Rohan Goddard, Lijun Zhang* and Xiaohua Xia

Department of Electrical, Electronic and Computer Engineering, University of Pretoria, Pretoria 0002, South Africa

Abstract

When sizing distributed hybrid renewable energy systems (HRESs) it has been found that capital costs can significantly be reduced when socio-demographic factors are considered. Unique electricity usage patterns have previously been classified using users' socio-demographic factors and used to optimize the size of individual stand-alone HRESs. An optimization model is formulated where an individual HRES is assigned to each of the six socio-demographic classifications and power sharing is implemented with neighboring sites in a specific configuration. Solving the optimization problem with a hybrid approach using Matlab's genetic algorithm and fmincon results in an 82,10% reduction in capital costs compared to the system without power sharing.

Keywords: Hybrid renewable energy system; Sizing; Optimization; Power sharing; Socio-demographic factors

1. Introduction

One of the big challenges with renewable energy sources such as photovoltaics (PV) and wind turbine generators (WG) is their stochastic generation characteristics [1]. By connecting different renewable energy sources together with

* Corresponding author. Tel.: +27 012 420 2674; fax: +27 012 362 5000.
E-mail address: lijun.zhang@up.ac.za

10.1016/j.egypro.2019.01.005

non-renewable sources and energy storage systems (ESSs) to create a hybrid power system helps to smooth out the generation of energy and also improves overall reliability of the power being supplied to users [2]. There is thus a strong motivation towards developing hybrid renewable energy systems (HRESs) and exactly why so much research has gone into planning and designing such systems to provide sustainable, cost effective and reliable forms of power generation [3]. When sizing a HRES, localized socio-demographic factors effecting the load demand profile need to be considered as it has been found in [4] to have a significant influence on the resultant cost of a standalone system. Sharing power between neighboring generating units has the potential to further reduce size of individual components resulting in further reduction in total installed system cost. However not much research has been done in this regard to combine the advantages of considering socio-demographic factors and sharing power between neighboring HRESs. This paper aims to fuse both, socio-demographic factors and power sharing in an attempt to further reduce total system cost.

2. Optimization model

2.1. Problem statement

When optimally sizing the components of an HRES, the site specific load profile is very important and will dictate the resultant cost [4]. Many different external and internal factors may influence the load profile such as seasonal variations and socio-demographic characteristics of the users [5]. Considering the large impact of socio-demographic factors on the load profile, [5] noted how the demand can be classified into six average hourly profiles. The seasonal variation is also contained in these six profiles because monthly average-daily load profiles were used to compile the classification. The temporal peak demand positions are all slightly different for all six classifications, some having only a single peak while others may have multiple. The six load profile classifications can be seen in Fig. 1.

In this study it is decided to create an individual HRES site for every type of load profile. Power sharing between neighboring HRESs is implemented in an effort to reduce the total installed system cost. This is compared to a base case where power sharing is not implemented. Costs associated with connecting HRES are not considered as it would be reasonable to assume an existing transmission grid system is already installed in a larger metropolitan area. Power sharing is considered for a fully connected HRES configuration, where all HRESs are electrically connected to each other as shown in Fig. 2. Power sharing is given by $P_{s,i\rightarrow j}(k)$ where i and j each refers to a particular HRES site and the arrow denoting power flow convention, e.g. $P_{s,1\rightarrow 2}(k)$ will be positive if power is flowing from HRES 1 to 2 and negative if power is flowing from HRES 2 to 1.

2.2. Objective function

The objective is to minimize the total capital cost of the distributed HRES. The socio-demographic and environmental factors at each HRES site (n) is incorporated in the model for a total of six HRES sites (N_{sites}). To achieve this, the following objective function is presented.

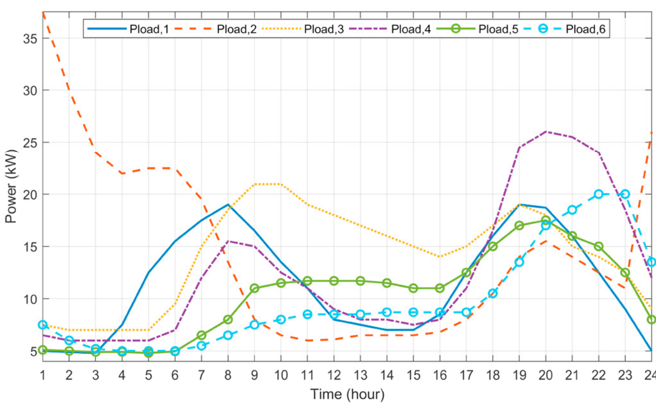

Fig. 1. Power demand for every HRES site.

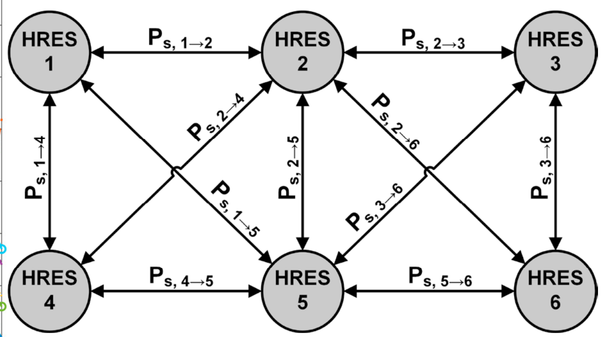

Fig. 2. Fully connected power sharing configuration

$$\min f(\mathbf{x}) = C_{PV}\left[\sum_{n=1}^{N_{sites}} N_{P,n}N_{S,n}\right] + C_{WG}\left[\sum_{n=1}^{N_{sites}} N_{WG,n}\right] + C_{Bat,cost}\left[\sum_{n=1}^{N_{sites}} C_{Bat,n}\right] + C_{Gen}\left[\sum_{n=1}^{N_{sites}} P_{Gen,\max,n}\right], \tag{1}$$

where C_{PV} is the cost of solar PV panel [\$/unit], $N_{P,n}$ and $N_{S,n}$ is the number of installed parallel and series solar PV panels respectively, C_{WG} is the cost of WG unit [\$/unit], $N_{WG,n}$ is the number of installed WG, $C_{Bat,cost}$ is the cost of deep cycle lead-carbon battery [\$/Wh], $C_{Bat,n}$ is the amount of installed battery capacity [Wh], C_{Gen} is the cost of diesel generator [\$/W] and $P_{Gen,max,n}$ is the installed diesel generator capacity [W]. The costs per unit (C_{PV}, C_{WG}) and per maximum capacities ($C_{Bat,n}$, C_{Gen}) were assumed constant for any installed quantity or capacity at all N_{sites}, this was done to ensure uniformity between the case study presented by Tito et al [4] and the case study of this work for easy comparison. It is also assumed that the PV panels, batteries, etc to be installed at each site are of the same specification and cost.

2.3. Decision variables

The optimization model consists of various decision variables, which are arranged into a decision vector shown in (2). Time is denoted by the index k which is an hourly interval, $k \in [1, 24]$ unless stated otherwise.

$$\begin{aligned}\mathbf{x}^T = \big[& N_{P,1}\cdots N_{P,N_{sites}} \quad N_{WG,1}\cdots N_{WG,N_{sites}} \quad C_{Bat,1}\cdots C_{Bat,N_{sites}} \quad P_{Gen,\max,1}\cdots P_{Gen,\max,N_{sites}} \\ & P_{S,j\to i}(k)\cdots P_{S,i\to j}(k) \quad P_{Gen,1}(k)\cdots P_{Gen,N_{sites}}(k) \quad P_{Bat,1}(k)\cdots P_{Bat,N_{sites}}(k)\big]\end{aligned} \tag{2}$$

where $P_{Gen,n}(k)$ is power produced by diesel generator and $P_{Bat,n}(k)$ is power supplied/absorbed by battery system. The battery power decision variable $P_{Bat,n}(k)$ is used to control the power flowing to and from deep cycle lead-carbon battery ESS.

2.4. Constraints

2.4.1. Power management constraints

Power balance constraint to ensure the load demand is fully satisfied at all times while utilizing power sharing is given in (3). The power required by the load at HRES site n during the time interval k is given by $P_{load,n}(k)$, $P_{PV,n}(k)$ is power produced by PV, $P_{WG,n}(k)$ is power produced by WG, $P_{Gen,n}(k)$ is power produced by diesel generator, $P_{Bat,n}(k)$ is power supplied/absorbed by battery system. Efficiency of connected converters at each power generating unit is given by $\eta_{PV,n}$ for PV, $\eta_{WG,n}$ for WG, $\eta_{Gen,n}$ for diesel generator and $\eta_{Bat,n}$ for ESS.

$$P_{load,n}(k) = \eta_{PV,n}P_{PV,n}(k) + \eta_{WG,n}P_{WG,n}(k) + \eta_{Gen,n}P_{Gen,n}(k) - \eta_{Bat,n}P_{Bat,n}(k) + P_{s,n}(k), \tag{3}$$

where the total power shared at site n, during time interval k is given by $P_{s,n}(k)$, which is calculated by adding all power inflows $P_{s,i\to j}(k)$ and subtracting all power outflows $P_{s,j\to i}(k)$, given efficiency of sharing ($\eta_{s,i\to j} = \eta_{s,j\to i}$) as shown in (4).

$$P_{s,n}(k) = \sum_{i=1,j=n,i<j}^{N_{sites}} \eta_{s,i\to j}P_{s,i\to j}(k) - \sum_{i=1,j=n,i>j}^{N_{sites}} \eta_{s,j\to i}P_{s,j\to i}(k), \;\; \forall\, n \in [1, N_{sites}],\; \forall\, k \in [1, 24] \tag{4}$$

2.4.2. PV power supply constraints

Detailed model of PV panel to obtain the maximum power production $P_{PV,input,n}(k)$ [W] given the number of series N_{sc} and parallel N_{pc} cells, open circuit voltage $V_{OC,n}(k)$ [V], short circuit current $I_{SC,n}(k)$ [A] and fill factor $FF(k)$ is used to determine the power produced by the PV system, as given by (5) [4].

$$\begin{aligned} P_{PV,input,n}(k) &= N_{sc} \times N_{pc} \times V_{OC,n}(k) \times I_{SC,n}(k) \times FF(k), \\ V_{OC,n}(k) &= V_{OC-STC} - K_V \times T_{c,n}(k), \\ I_{SC,n}(k) &= \left(I_{SC-STC} + K_I \times [T_{c,n}(k) - 25°C]\right) \times G_n(k)/1000, \\ T_{c,n}(k) &= T_A + \left(NOCT - 20°C\right) \times G_n(k)/800, \end{aligned} \tag{5}$$

where $T_{c,n}(k)$ [°C] is the cell temperature, T_A ambient temperature fixed at 25°C, normal operating cell temperature (*NOCT*) is taken from manufacturers specification, $G_n(k)$ [W/m^2] global solar irradiance, $I_{SC\text{-}STC}$ short circuit current under standard test conditions, K_I current temperature coefficient, $V_{OC\text{-}STC}$ open circuit voltage under standard test conditions and K_V voltage temperature coefficient.

The total power produced $P_{PV,n}(k)$ [W] by the installed PV array at each site (n) is a function of power produced per panel $P_{PV,input,n}(k)$, the efficiency of the panel (η_{PV}), amount of series ($N_{S,n}$) and parallel ($N_{P,n}$) solar panels. See Table 1. for all PV coefficients and specifications.

$$P_{PV,n}(k) = \eta_{PV} \times N_{S,n} \times N_{P,n} \times P_{PV,input,n}(k), \; \forall \; n \in [1, N_{sites}], \; \forall \; k \in [1, 24] \tag{6}$$

Table 1. Solar PV panel specifications.

$N_{sc} \times N_{pc}$	$FF(k)$	$V_{OC\text{-}STC}$ [V]	$V_{SC\text{-}STC}$ [A]	K_V [%/°C]	K_I [%/°C]	$NOCT$ [°C]	η_{PV} [%]	$N_{s,n}$	C_{PV} [\$/unit]
6	0.7658	38	9.45	-0.31	0.053	45	16.8	2	640

2.4.3. WG constraints

The specific power output $P_{WG,input,n}(k)$ [W/m^2] of WG is dependent on the wind speed $v_n(k)$ [m/s] at each HRES site n [4]. Firstly the wind speed needs to be calibrated from the measured height ($h_{ref,n}$) to the hub height ($h_{installed,n}$) of the installed WG, with a friction coefficient equal to the open space (α_n=1/7) by (7) [6]. Power produced by the WG is also dependent on specifications of the wind turbine such as the cut-in $v_{ci,n}$, cut-out $v_{co,n}$ and rated $v_{r,n}$ wind speeds given by (8). The WG specifications are given in Table 2.

$$v_n = v_{ref,n} \left[h_{ref,n} / h_{installed,n} \right]^{\alpha_n} \tag{7}$$

$$P_{WG,input,n}(k) = \begin{cases} 0 & \text{if} \quad v_n(k) < v_{ci,n}, \\ \dfrac{P_{WG,rating,n}}{v_{r,n}^3 - v_{ci,n}^3} v_n^3(k) - \dfrac{v_{ci,n}^3}{v_{r,n}^3 - v_{ci,n}^3} P_{WG,rating,n} & \text{if} \quad v_{ci,n} \leqslant v_n(k) < v_{r,n}, \\ P_{WG,rating,n} & \text{if} \quad v_{r,n} \leqslant v_n(k) < v_{co,n}, \\ 0 & \text{if} \quad v_n(k) \geqslant v_{co,n}, \end{cases} \tag{8}$$

Finally the output power $P_{WG,n}(k)$ [W] produced by the WG at each site (n), which is a function of the efficiency of the WG (η_{WG}), total swept area (A_{WG}) and number of installed WG $N_{WG,n}$, is given by (9).

$$P_{WG,n}(k) = \eta_{WG} \times A_{WG} \times P_{WG,input,n}(k) \times N_{WG,n}, \; \forall \; n \in [1, N_{sites}], \forall \; k \in [1, 24] \tag{9}$$

Table 2. WG specifications.

$h_{ref,n}$ [m]	$h_{installed,n}$ [m]	$P_{WG,rating,n}$ [W]	$v_{ci,n}$ [m/s]	$v_{r,n}$ [m/s]	$v_{co,n}$ [m/s]	η_{WG} [%]	A_{WG} [m^2]	C_{WG} [\$/unit]
10	30	1000	2.5	10.5	30	90	5.8	2400

2.4.4. Diesel generator constraints

Constraints related to the correct operation of the diesel generators is given here. Note the generator is sized using the maximum demand required by the diesel generator throughout the day.

$$P_{Gen,\max,n} \geqslant P_{Gen,n}(k), \text{ for } \forall\, n \in [1, N_{sites}] \text{ and } \forall\, k \in [1, 24] \tag{10}$$

The ramp rates of the generator should also be constrained to limit the up (UR_n =20 kW/Δk) and down (DR_n = 20 kW/Δk) ramp rates respectively, for each HRES site (n). The cost per installed diesel generator was inflated above the nominal cost to include a penalty for emissions such as carbon dioxide (CO_2), carbon monoxide (CO), sulphur dioxide (SO_2) and nitrogen oxides (NO_x) [7]. The cost per watt installed diesel generator is given by, C_{gen} = 1000 $/kW [8]. A multi-objective optimization would have been an alternative approach but would have immensely increased the complexity.

$$-DR_n \leqslant \left[P_{Gen,n}(k) - P_{Gen,n}(k-1)\right]/\Delta k \leqslant UR_n, \ \forall\, n \in [1, N_{sites}], \ \forall\, k \in [2, 24] \tag{11}$$

2.4.5. Battery system constraints

The charging/discharging power of the battery $P_{bat,n}(k)$ is controlled through the capacity of the installed deep cycle lead-carbon batteries (C_{bat}) and was set to a maximum limit of 50% of the total installed battery capacity divided by a single time interval (Δk), which is one hour [9]. The depth of discharge (DOD) was set at 50% to strike a balance between longevity of battery lifetime and maximizing operational capacity [10].

$$\begin{array}{llll} [DOD/100](C_{bat}) & \leqslant SOC_{Wh,n}(k) & \leqslant C_{bat}, & \forall\, n \in [1, N_{sites}], \ \forall\, k \in [1, 24] \\ -0.5C_{bat}/\Delta k & \leqslant P_{Bat,n}(k) & \leqslant 0.5C_{bat}/\Delta k, & \forall\, n \in [1, N_{sites}], \ \forall\, k \in [1, 24] \end{array} \tag{12}$$

The batteries were initialized to 80% state of charge (SOC) and another constraint was included to ensure repeated operation of the HRES. The costs associated to the capital and installation costs of the deep cycle lead-carbon batteries, $C_{Bat,cost}$ = 289 $/kWh [4].

$$SOC_n(1) = SOC_n(24), \quad \forall\, n \in [1, N_{sites}] \tag{13}$$

3. Results

3.1. Hybrid optimization algorithm

Because the problem is essentially a NP-hard integer programming problem it is solved by a hybrid algorithm approach using Matlab's optimization toolbox [11]. The genetic algorithm (GA) was used to firstly obtain the approximate location of the global minimum, thereafter fmincon's interior-point algorithm was used to accurately locate the exact optimum solution. Thereafter $N_{P,n}$ and $N_{WG,n}$ are rounded up to the nearest integer. GA with a population size of 100 was used and run for a maximum of 2000 generations or until average cumulative change in objective function (f) is less than function tolerance (1×10^{-6}) and constraint violation is less than chosen constraint tolerance (1×10^{-3}). Thirty optimization runs of both scenarios, power sharing disabled and power sharing enabled were completed with final capital cost having a coefficient of variance (cv) cv_{share}=2.40% for power sharing enabled and $cv_{no\text{-}share}$=0.00% for sharing disabled. Thus the difference between subsequent runs are negligible.

3.2. Evaluation of the results

From the results shown in Table 3 it is evident that sharing power between neighboring HRES sites can contribute to large cost savings. Implementing power sharing allowed for an 82.10% reduction in total system cost. Total cost was reduced by decreasing the size of all installed generating units while still being able to satisfy the load at each site. On average the numbers of PV panels were reduced by 61%, average installed swept area of WG was reduced by 80%, battery capacity was reduced by 85% and the average size of installed diesel generator was reduced by 79%. In the power sharing disabled scenario, site 1 was optimized to install a large battery and generator only, which at first might seem counterintuitive. However because peak power demand does not coinciding with either peak irradiance levels (nominally during midday) or rated wind speeds the optimization favored resulted in a more expensive approach to satisfy the load at HRES site 1. When sizing individual isolated HRES, much more diesel generators were installed to satisfy user demand during peak demand periods, considerably increasing the capital cost.

Table 3. Optimal sizing of HRES results with and without sharing.

	Power sharing enabled					Power sharing disabled				
Total cost [$]	307 022					1 703 496				
Hybrid renewable energy system number	$N_{P,n} \times N_{S,n}$ [units]	$N_{WG,n}$ [units]	$A_{WG,n}$ [m^2]	$C_{bat,n}$ [kWh]	$P_{gen,max,n}$ [kW]	$N_{P,n} \times N_{S,n}$ [units]	$N_{WG,n}$ [units]	$A_{WG,n}$ [m^2]	$C_{bat,n}$ [kWh]	$P_{gen,max,n}$ [kW]
HRES 1	4	1	5.80	59.03	34.92	0	0	0	960.43	279.75
HRES 2	2	3	17.40	59.07	17.31	10	13	75.40	306.88	279.75
HRES 3	2	1	5.80	58.95	31.88	2	16	92.80	253.85	8.14
HRES 4	2	1	5.80	58.78	35.36	10	9	52.20	423.52	9.07
HRES 5	2	2	11.60	59.46	36.99	0	8	46.40	224.93	9.23
HRES 6	2	1	5.80	59.37	14.60	14	1	5.80	332.54	254.32

4. Conclusion

Sharing power between HRES sites can be very effective in cost savings as demonstrated by the results of this study, namely 82.10% of savings. However, savings will significantly be reduced if there is no transmission grid already installed that can be relied upon. The power sharing scheme utilized in this paper is only a single configuration and offers the best connection between sites. Existing grids are not necessarily connected in such an ideal interconnected scheme and may rather be connected in a centralized, ring or many other configurations. Power sharing schemes may not offer such a large cost saving thus many other power sharing schemes should be investigated while still considering socio-demographic factors.

References

[1] Khare V, Nema S, Baredar P. Solar-wind hybrid renewable energy system: A review. Renewable and Sustainable Energy Reviews. 2016;58:23–33.
[2] Fathima AH, Palanisamy K. Optimization in microgrids with hybrid energy systems - A review. Renewable and Sustainable Energy Reviews. 2015;45:431–46.
[3] Olatomiwa L, Mekhilef S, Ismail MS, Moghavvemi M. Energy management strategies in hybrid renewable energy systems: A review. Renewable and Sustainable Energy Reviews. 2016;62:821–35.
[4] Tito SR, Lie TT, Anderson TN. Optimal sizing of a wind-photovoltaic-battery hybrid renewable energy system considering socio-demographic factors. Solar Energy. 2016;136:525–32.
[5] Stoecklein A, Pollard A, Camilleri M, Tries J, Isaacs N. The household energy end-use project: measurement approach and sample application of the New Zealand household energy model. In: CIB World Build Congr. Wellington, New Zealand; 2001.
[6] Masters GM. Renewable and Efficient Electric Power Systems. Wiley IEEE Press; 2013.
[7] Moradi MH, Eskandari M, Showkati H. A hybrid method for simultaneous optimization of DG capacity and operational strategy in microgrids considering uncertainty in electricity price forecasting. Renewable Energy. 2014;68:697–714.
[8] Hong YY, Lian RC. Optimal sizing of hybrid wind/PV/diesel generation in a stand-alone power system using markov-based genetic algorithm. IEEE Transactions on Power Delivery. 2012;27(2):640–7.
[9] Chen SX, Gooi HB, Wang MQ. Sizing of energy storage for microgrids. IEEE Transactions on Smart Grid. 2012 Mar;3(1):142–51.
[10] Yang H, Lu L, Zhou W. A novel optimization sizing model for hybrid solar-wind power generation system. Solar Energy. 2007;81(1):76–84.
[11] MathWorks. Matlab optimization toolbox user's guide [Internet]. 2018 [cited 2018 Jul 26]. p. 1172. Available from: https://www.mathworks.com/help/pdf_doc/optim/optim_tb.pdf